Smart Sensors for Demand Response

Vincenzo Paciello, *Senior Member, IEEE*, Antonio Pietrosanto, *Senior Member, IEEE*, and Paolo Sommella, *Member, IEEE*

***Abstract*— Smart Grid is being proposed as a prime solution for the effective growth of electricity market allowing the heterogeneous players to assume real-time autonomous reactions to the changing conditions of the grid and new services (such as demand response, DR, and vehicle-to-grid, V2G) to be introduced. One of the main requisite for such development is represented by advanced metering infrastructure (AMI) which typically provides timely and reliable information about the smart grid. This paper introduces an innovative first block of the AMI represented by a smart sensor based on ARM architecture. The prototype is described in terms of both the hardware and software features and the metrological characterization is provided through the experimental test according to OIML R-46.**

***Index Terms*— Smart sensors, IEEE 1451, AMI, demand response, open metering.**

I. Introduction

THE increasing demand of energy and the availability of renewable/distributed energy sources are turning the static centralized electrical network into a flexible, living, and proactively operating infrastructure known as Smart Grid. Although proactive control techniques are currently being developed, because of the uncertainty intrinsic in load forecasting, Demand Management seems to be yet the most successful solution, especially where a liberalized and competitive market is limited by transmission constraints. In such cases, the elasticity of demand that helps to reduce the load peaks relieves the whole electrical system in terms of both energy generation and network congestion. In order to provide an elastic behavior the main efforts were addressed to short-term demand ([1], [2]).

Demand Response (DR) [3]–[6], provides a chance for users to play a significant role in the operation of the electric grid by reducing or shifting their electricity usage during peak periods in response to time-based rates or other forms of financial incentives. In more details, the demand response programs (carried out by some electric system planners and operators for balancing supply and demand) include offering time-based rates such as time-of-use pricing, critical peak rebates, real time pricing, variable peak pricing, and critical peak pricing. DR includes direct load control programs which provide the ability for power companies to cycle air conditioners and water heaters on and off during periods of peak demand in exchange for a financial incentive and lower electric bills.

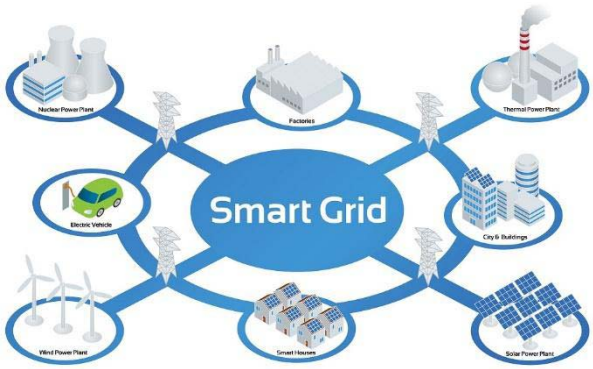

Fig. 1. The concept of Smart Grid.

Although the quantification of (economic, financial and social) benefits coming from flexibility and the determination of which parameters have to be taken into account (according to specific market, country and consumers community) are still debated ([7], [8]), the expected results from Demand Side Management is a participatory network (see Fig. 1) in which all market participants share responsibilities as well as benefits [9]–[12]. Utilities will be able to better manage peak demand and schedule intervention on network to avoid congestion, whereas end users may optimize their own consumption according to real-time prices and individual needs by offset power bills.

One of the main requirements of this scenario is the actual availability of Smart Sensors able to provide all relevant users of the energy conversion chain the bidirectional data communication to/from the system operator.

Starting from previous experiences in the field of remote metering and wireless sensor networks [13]–[17], the authors proposed in [18] a prototype of low-cost smart meter, as basis of an Advanced Metering Infrastructure (AMI) for Demand Side Management (DSM).

In the present study, an original solution to provide accurate power and energy measurements is described when the frequency oscillations and non- sinusoidal electric currents have to be faced. Thus, the paper is organized as follows: after a brief review of the network architecture, the Smart Sensor is disclosed in terms of the main hardware and software features thanks to which the calculation of both time and frequency domain metrics are implemented for the electrical power measurements. Finally, the experimental verification according to OIM R46 [19] both in sinusoidal and distorted conditions are reported and discussed.

Manuscript received April 3, 2017; revised May 22, 2017 and June 29, 2017; accepted June 29, 2017. Date of publication July 20, 2017; date of current version November 10, 2017. The associate editor coordinating the review of this paper and approving it for publication was Dr. Rosario Morello. *(Corresponding author: Vincenzo Paciello.)*

V. Paciello is with the Department of Electrical and Information Engineering "Maurizio Scarano", University of Cassino and Southern Lazio, 03043 Cassino, Italy (e-mail: v.paciello@unicas.it).

A. Pietrosanto and P. Sommella are with the Department of Industrial Engineering, University of Salerno, 84084 Fisciano, Italy (e-mail: apietrosanto@unisa.it; psommella@unisa.it).

Digital Object Identifier 10.1109/JSEN.2017.2728611

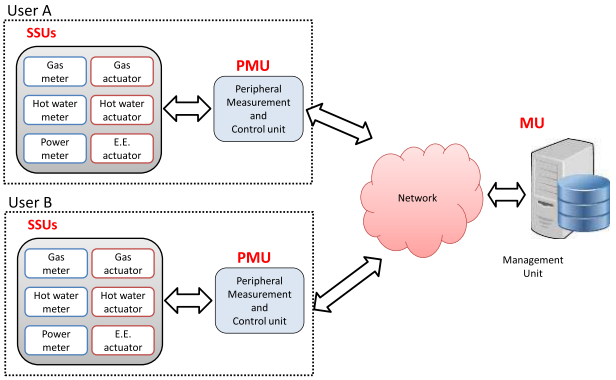

Fig. 2. Proposed smart metering and actuation architecture.

II. AMI FOR DSM

A. Overview

According to the scheme proposed for AMI [20], [21], and depicted in Fig. 2 a Peripheral Measurement and communication Unit (PMU) is connected to multiple Smart Sensor Units (SSUs), each one devoted to detect the consumption of electrical energy, gas and hot water respectively. Main tasks of the PMU are represented by data collection from the SSUs and computation of the corresponding statistics and quality metrics.

Different PMUs may be connected to a Management Unit (MU), thus constituting a suitable network, which may include multiple branches, able to match the energy application needs of university campus, great enterprise and/or hospital where the various departments are typically served by different lines.

The MU is devoted to: i) reception of the market prices, information about the line congestion and the energy availability from the Independent System Operator (ISO); ii) transmission (towards the PMUs) of information and commands about load curtailments concerning with the end users (subscribers of suitable supply contracts). As to the latter features, the load curtailment procedures [22] need the adoption of suitable actuators. In detail, such devices may be integrated into the proposed scheme at the same level as the SSUs, once the communication bus (to the PMU) is provided as bidirectional (upward link for measurements transmission and downlink for the actuation commands).

Finally, the MU may be also adopted for the Distributed Generation, allowing each end users to sell their own energy surplus on the market. Thus, the MU may actually provide the cheaper solution to the user and at the same time allows the ISO to cut down absorption peaks.

B. System Specifications

The proposed metering architecture has been designed by taking into account the following requirements:

- a target function has been introduced to develop a suitable strategy for optimizing consumption on the basis of the field data. The model will use both measured data (electrical power, gas flow) and other grid operation information such as weather forecast;
- the MU should be implemented on a conventional workstation, providing interaction with the ISO and execution of DSM actions. The MU should also include a web interface, by allowing end users to know real-time updates in energy consumptions and corresponding bill;
- the PMU should be implemented as an embedded system (based on microcontroller) able to collect data from multiple SSUs, and determine a "synthetic energy consumption figure" to be sent to the MU. In detail, the computation of statistics about the users as well as the extraction of "Power Quality indices" about the electrical energy are requested. Finally, the PMU should implement gateway functionality about the DSM commands (issued by the MU and directed to the actuators);
- The SSU should be based on the IEEE 1451 standard [23] providing basic signal processing capabilities, needed to compute RMS values, active and reactive power, and format data according to the communication protocol. A suitable communication module should be included for interaction with the data bus, which may rely on different mediums and different standards, according to the environment and the convenience;
- Actuators able to reduce the corresponding electrical, gas and hot water flows should be placed at the same level as SSUs, and provided with suitable communication modules that allow the commands from MU be received through the PMUs.

III. THE SMART METER

A. Hardware

The Electrical Energy SSU and the PMU have been integrated into a single prototypical device based on an ARM microcontroller STM32F103RE, in order to achieve a good compromise between computational capabilities, energy consumption and low cost technology, whereas the hot water and gas meter are connected directly to the microcontroller (see Fig. 3). From a physical point of view, each meter consists of the: processing section, level adapters, transduction section composed by voltage and current sensors, the RS232 port for communication, one proportional actuator and three relays (that permit to manage some loads).

In the following, the main functions executed by the microcontroller are detailed:

- real time signal acquisition,
- network communication,
- computation of power measurements metrics.

B. Data Acquisition Software

According to the developed firmware, the microcontroller is able to decode the digital signal from the hot water meter and directly manage (via its internal ADCs) the analog output from gas, voltage and electric current transducers. In detail, a sampling frequency equal to 10 kHz is adopted over an "observation period" of 5 seconds. The following parameters about the electrical quantities are computed: average and RMS values of electric current and voltage; active, apparent and reactive power; maximum active, apparent and reactive power;

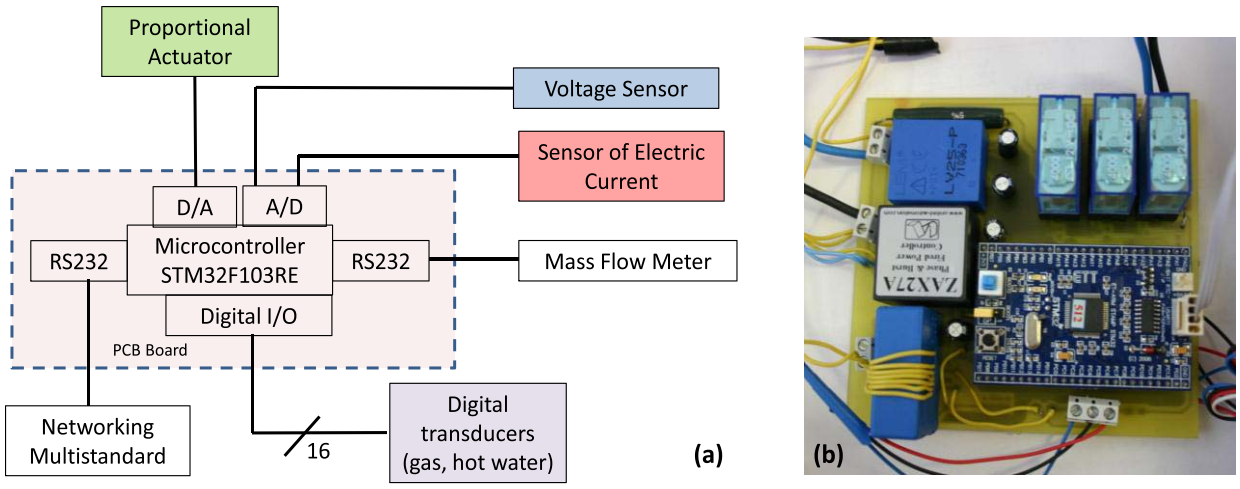

Fig. 3. Smart meter: Bloc diagram of the architecture (a) and a image of the prototype (b).

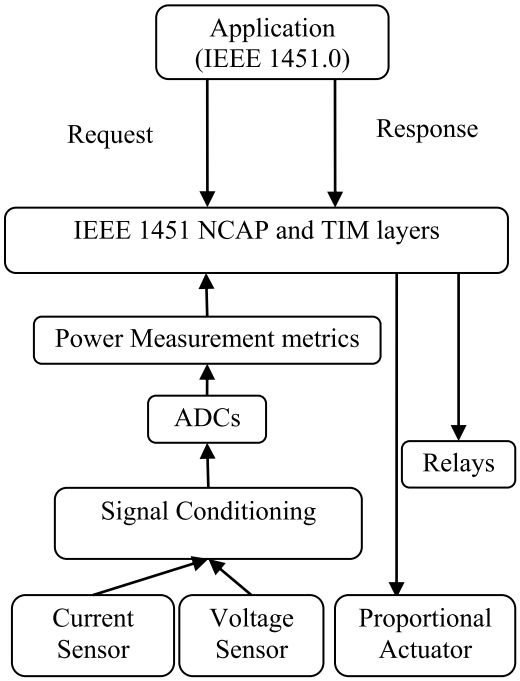

Fig. 4. The Meter Interface.

active, apparent and reactive energy. About the gas and hot water, difference of temperature (for the latter) and volume (for both of them) are monitored.

C. Communication Software

The meter is based on standard IEEE 1451 [24]. A software module was implemented to add the TIM and the NCAP capability to meter. Fig. 4 shows the IEEE 1451 standard interface implemented on the meter. The application may call some services using the APIs. The purpose of the APIs is to simplify the applications on the TIMs. The authors have implemented the interface for applications, which is a set of request/response pairs or application programming interface (API). The most important services are: initialize, read data, set the state of the relays and set the output of the proportional actuator. For each services, a microcontroller task has been implemented. The microcontroller executes the measurement task and waits on communication channel for incoming request.

D. Power Measurement Metrics

As far as the measure of the electrical energy, the proposed smart meter can be included in a modern class of meters called static meters. They are based on the analog to digital conversion of voltage and electric current signals and their numeric processing. By means of measurement algorithms (identified as metrics), applied on voltage and electric current signals, the quantities of interest (i.e. power, energy, etc…) are retrieved.

A complication in this context is represented by the presence of non-sinusoidal signals of both voltage and electric current signals. Indeed, the more and more widespread nonlinear loads and power electronics represent the main source of phenomena such as harmonic distortion, dips and swells, noise which makes the signals existing on the electrical network significantly different from the ideal sinusoidal ones. While active and reactive power in sinusoidal conditions are clearly defined according to the corresponding physical significance, different interpretations have been proposed in literature about non-sinusoidal signals. Some authors suggest a mathematical extension of definitions held for sinusoidal signals through the introduction of additional terms (without corresponding physical significance), but make up for the incoherence of applying mathematical formulation intended for sinusoidal signals to distorted waveforms. Other authors retain the physical meaning discarding previous mathematical descriptors. Obviously, different definitions lead to different means of calculation both in time and frequency domain. A review of main contributions may be found in [25]–[29].

With the aim of giving answers on this field, in the year 2010 and in 2012, after about one decade of scientific discussion from the first draft publication, the last version of the standard [19] was issued. It provides definitions of electric power to quantify the flow of electrical energy in single phase

and three-phase circuits under sinusoidal, non-sinusoidal, balanced and unbalanced conditions. Two possible domains (time and frequency) for the power calculation are adopted. The suggested power definitions, where the preferred mathematical expressions recommended for the instrumentation design are marked with a || symbol, are reported in the following.

The metric for the calculation of the active power in the time domain is:

$$||P = \frac{1}{\mathbf{k}T}\int_{\tau}^{\tau+\mathbf{k}T} \upsilon i \; dt \tag{1}$$

The time from τ to τ+kT is the observation time interval, where τ is the instant when the time starts, k is an integer number and T=1/frequency is the cycle of the fundamental frequency; υ and i are the instantaneous voltage and electric current respectively.

The metric for the calculation of the active power in the frequency domain is:

$$P = \mathrm{P_1}+\mathrm{P_H} \tag{2}$$

where $\mathrm{P_1}$ is the fundamental active power that is often referred to the fundamental frequency

$$||P_1 = \frac{1}{\mathbf{k}T}\int_{\tau}^{\tau+\mathbf{k}T} \upsilon_1 i_1 \; dt = V_1 I_1 \; \cos\varphi_1 \tag{3}$$

and $\mathrm{P_H}$ is the harmonic active power (non fundamental active power)

$$P_H = V_0 I_0 + \sum_{\mathrm{h}\neq 1} V_h I_h \cos\varphi_h = \mathrm{P}-\mathrm{P_1}|| \tag{4}$$

υ_1,i_1 are the fundamental instantaneous voltage and electric current, and $\mathrm{V_1}$, $\mathrm{I_1}$ their root mean square (RMS) values while φ_1 is the phase angle between them. $\mathrm{V_0}$, $\mathrm{I_0}$ are the continuous component of voltage and electric current and $\mathrm{V_h}$ and $\mathrm{I_h}$ are the RMS values of the h-harmonic components of voltage and electric current while φ_h is the phase angle between them. It is important to note that P_H, as defined, contains also components for which h is not an integer (i.e. interharmonics and subharmonics).

The fundamental reactive power is defined as:

$$||Q_1 = \frac{\omega}{\mathbf{k}T}\int_{\tau}^{\tau+\mathbf{k}T} i_1 \left[\int \upsilon_1 dt\right] dt = V_1 I_1 \; \sin\varphi_1 \tag{5}$$

where $\omega = 2\pi\,\mathrm{f}$ and f is the fundamental frequency.

As far as the apparent power:

$$||S = \mathrm{VI} \tag{6}$$

where V and I are the RMS values of the voltage and electric current respectively.

Finally, it is defined the non-active power that lumps together both fundamental and non fundamental non active components:

$$||N = \sqrt{\mathrm{S}^2 - \mathrm{P}^2} \tag{7}$$

The non-active power N must not be confused with a reactive power. Only when the waveforms are perfectly sinusoidal, $N = Q_1 = Q$ is true.

Starting from the above standardized metrics, both time and frequency domain can be eligible for the measurement of electrical power. Considering that the time domain approach needs less processing resource and represents the preferred mathematical expressions recommended for the instrumentation design, the power metrics reported in equations (1) and (7) are considered and implemented on the ARM microcontroller.

An ancillary method is adopted to retrieve information about the sign of non-active power: the electric current and voltage waveform at the fundamental frequency (hereinafter assumed equal to 50 Hz, nevertheless validity is held for 60 Hz with slight modification) are considered. According to the phase angle between voltage and electric current, the direction of the power flow is obtained. Executing the Goertzel algorithm [30] at the fundamental frequency, voltage and electric current are transposed into the frequency domain:

$$V\,(k) = Re_V + jIm_V = V_0 e^{j\alpha} \tag{8}$$

$$I\,(k) = Re_I + jIm_I = I_0 e^{j\beta} \tag{9}$$

$$V\,(k) = V_0[\cos\,(\alpha) + jsin(\alpha)] \tag{10}$$

$$I\,(k) = I_0[\cos\,(\beta) + jsin(\beta)] \tag{11}$$

Thus, it follows:

$$Re_V Re_I + Im_V Im_I = V_0 I_0 \cos\,(\alpha-\beta) = V_0 I_0 \cos(\varphi) \tag{12}$$

$$Re_V Im_I - Im_V Re_I = V_0 I_0 \sin\,(\alpha-\beta) = V_0 I_0 sin\,(\varphi) \tag{13}$$

The outputs of the Goertzel algorithm allow the sign of both active and non-active power to be retrieve for bidirectional measurements.

Obviously, the meter should also be able to follow the fundamental frequency variations introduced by load variation on the power grid (non-stationary condition), thus preserving the metrological performance.

To this end, for each observation period, the frequency of the fundamental is calculated and the sampling time is adjusted to adapt to the measured fundamental and guarantee synchronous sampling. Executing the Goertzel algorithm at five different frequencies (40 – 45 – 50 – 55 – 60 [Hz]), centered around the nominal value of the fundamental, five points in the frequency domain can be obtained (see the Appendix A).

An interpolation and analysis algorithm is then executed [31] to search for the maximum of the obtained lobe and find the desired frequency value (see the Appendix B). Being the acquisition from the ADCs triggered by an internal programmable timer, it is possible to obtain a synchronous sampling modifying the programmed interval between two trigger events accordingly to the previously determined frequency of the fundamental.

By means of an ad-hoc algorithm (implemented on ARM microcontroller), it is possible to follow the grid frequency variations and change the sampling frequency (resolution < 1 mHz) to minimize the error on the formula.

The procedure is illustrated in Fig. 5. The acquisition is such that each period of the signal 200 samples are acquired: the sampling frequency, adjusted to the determined fundamental frequency of the signal to comply to the requirement of synchronous sampling, is computed as the fixed number of samples per period multiplied by the

Fig. 5. Sampling frequency adjustment.

newfound fundamental frequency. The algorithm used to determine the sign is based on the Goertzel algorithm particularized at the fundamental frequency: it is updated at each observation period (5 s) with the correct frequency.

With respect to the widespread hardware PLL-based solution, the software lock on the fundamental frequency allows to keep low the device cost, without sacrificing performance. In conclusion, at each observation period (5 s), the following cycle is executed by the STM32F103 microcontroller: i) compute power quality indices i.e. THD, variation from nominal frequency; ii) multiply the mean values in the period of active power and non-active power by the period and sum them to the respective energy counters, iii) update the relative maximum and relative minimum values of active and non-active power and other consumption variables, iv) read the output of the digital transducers (gas and hot water); v) compute usage statistics; vi) read the command coming from the MU and update a 132 byte record of data output, vii) execute the command for the proportional actuator. About the last task, the command could be sent either from the ISO by the MU or issued automatically by the meter itself (DR) on the basis of the measured frequency to minimize the energy cost due to frequency fluctuations according to [22].

E. Measurement Software

The sample acquisition over the observation period is managed by the developed firmware via DMA, thus allowing the CPU to evaluate the quantities of interest each N samples. (indeed the time required for data processing is less than the time required for acquiring the N samples).

More in detail, the processing routine updates the following quantities:

i) voltage and electric current rms values:

$$V_{rms} = \sqrt{\frac{1}{N}\sum_{N} v^2(n)}; \quad I_{rms} = \sqrt{\frac{1}{N}\sum_{N} i^2(n)};$$

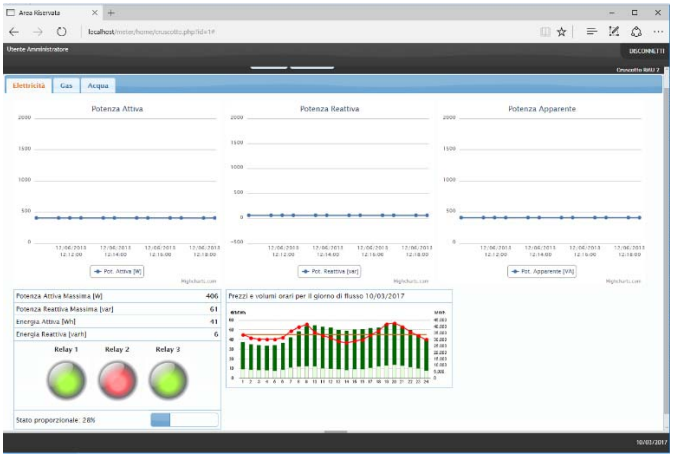

Fig. 6. The Screenshot of Management Unit Web page.

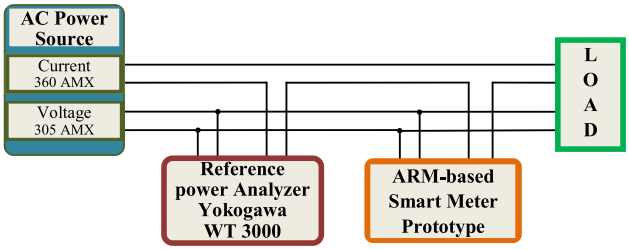

Fig. 7. The measurement set-up.

ii) active power: $P = \frac{1}{N}\sum_{N} v(n) \cdot i(n)$;

iii) the energy: $E = E_{previous} + P \cdot \Delta t$, where Δt is equal to N/fs;

iv) the apparent power, S, and the power factor, PF,

$$S = V_{rms} \cdot I_{rms}, \quad PF = \frac{P}{S};$$

v) the fundamental frequency (by means of Goertzel algorithm)

vi) the voltage and current components at the fundamental frequency, V_1, I_1 through interpolation algorithm;

vii) the non active power, with its sign

$$N = sign(N) \cdot \sqrt{S^2 - P^2};$$

viii) voltage and current Total Harmonic Distortion (THD_V and THD_I):

$$THD|_V = \frac{\sqrt{(V_{rms})^2 - \left(V_1^{rms}\right)^2}}{V_1^{rms}};$$

$$THD|_I = \frac{\sqrt{(I_{rms})^2 - \left(I_1^{rms}\right)^2}}{I_1^{rms}}.$$

If the fundamental frequency is changed the new sampling frequency is configured, as f_1/N.

IV. The Managent Unit

The MU is implemented on a conventional personal computer; the connection to the PMU represented by the microcontroller is realized through Wi-Fi, using a serial port as

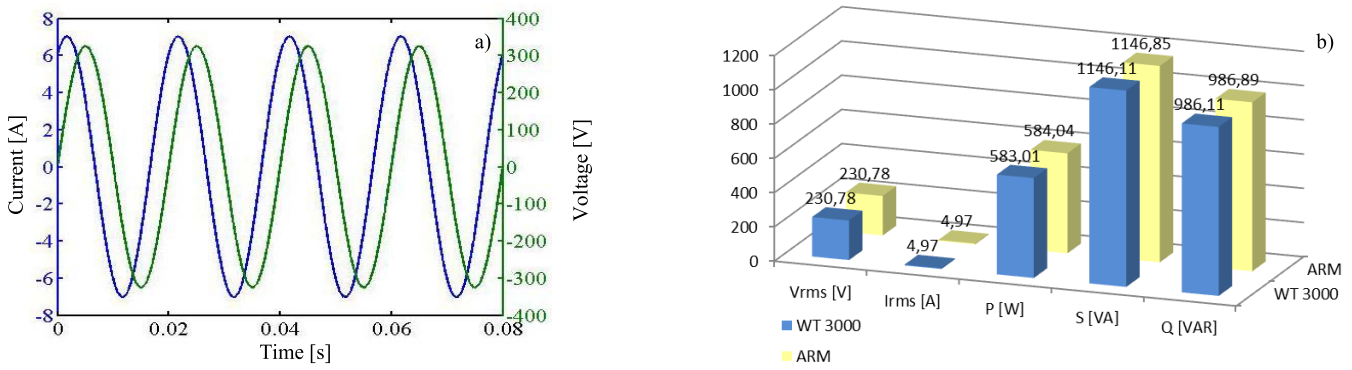

Fig. 8. Sinusoidal signals with no influence quantities: a) the considered voltage and electric current test signals and b) the corresponding obtained results.

output for the STM32F103 and a serial to Wi-Fi converter and a simple Wi-Fi receiver. The central system is based on a database for storing data, and a multi-user web interface to access the information. Two profiles were created for access to the system, through appropriate credentials: Administrator and User. The administrator can view the status of the entire network, while the user can view only their own information. As an example, the Fig. 6 shows the user profile screen. On the User screen, it is possible to view all the information relating to consumption, in particular, the Fig. 6 shows the states of the three lines that can be controlled remotely, and proportional actuator percentage. The red color indicates the disconnected line, while the green color indicates the connected line, for proportional actuator a blue slider bar is shown. The user can see the consumption both historical and current ones. The screen also shows a graph of the energy costs related to the previous day.

V. Experimental Results

For the metrological characterization of the developed meter the following measurement set-up has been employed (Fig. 7 shows the measurement set-up):

- AC power source system, provided by Pacific Power Source, mounted in a watt-hour configuration. It is assembled by two AMX 360 connected in parallel and an AMX 305 (for the electric current and voltage generation respectively) synchronized by means of a 4173 DMR link. It is able to generate two different arbitrary waveforms with a user defined phase shift allowing a maximum power of 12 kVA and 0.5 kVA (for the electric current and voltage respectively) over the 20 Hz – 5 kHz frequency band;
- Resistive Load;
- reference power analyzer, Yokogawa WT3000, that allows the measurement of the electrical parameters (electric current, voltage, active and reactive power and energy, power factor, etc…);
- the ARM-based Smart Meter prototype described in section III.

The test plan has been designed by taking into account the following standards:

- the Measuring Instrument Directive (MID) [32], which establishes the requirements that the meters, devices, and systems must satisfy when placed on the market and/or put into use for reasons of public interests, public health, public safety, public order, protection of the environment, protection of consumers, duty and tax levying and fair trading. It demands to the harmonized standards (technical specification adopted by CEN, CENELEC or ETSI prepared in accordance with the General Guidelines agreed between the Commission and the European standards organizations) a detailed explanation of the values and the test cases for the influence quantities, the disturbances and so on. In particular, the imposed test signals are defined in the standard [33].
- the draft document (OIML R-46) of the Organization International de Métrologie Légale on Active Electrical Energy Meters [18], which gives an easily-adoptable set of requirements and tests to meet the needs of the MID to the regulatory bodies.

Both the MID and the OIML R-46 documents have the same approach to the test of the energy meters and also the imposed test signals are substantially the same. Thus, the following test cases have been carried out for the experimental characterization of the realized smart meter.

1) Sinusoidal signals with no influence quantities (Figure 8a).
2) Harmonics in voltage and electric current circuits (Figure 9a) with: fundamental frequency electric current: $I_1 = 11.5$ A; fundamental frequency voltage: $V_1 = 230$ V; fundamental frequency power factor: 1; content of 5th harmonic electric current: $I_5 = 40\%$ of I1; content of 5th harmonic voltage: $V_5 = 10\%$ of V_1; 5th harmonic power factor: 1.
3) DC and even harmonics in the a.c. electric current circuit. The tests were performed considering a sinusoidal voltage and the electric current waveform, with a maximum value of 25 A, as shown in Figure 10a).
4) Odd harmonics in the a.c. electric current circuit. The tests were performed considering a sinusoidal voltage and the electric current waveform, with a maximum value of 5 A, as shown in Figure 11a).
5) Sub-harmonics in the a.c. electric current circuit. The tests were performed considering a sinusoidal voltage and the electric current waveform, with a maximum value of 5 A, as shown in Figure 12a).

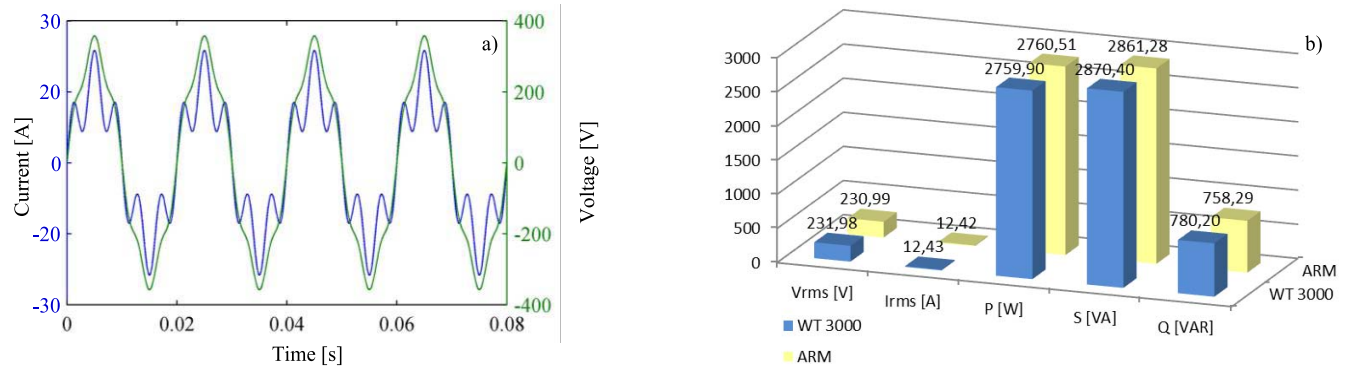

Fig. 9. Harmonics in voltage and electric current circuits: a) the considered voltage and electric current test signals and b) the corresponding obtained results.

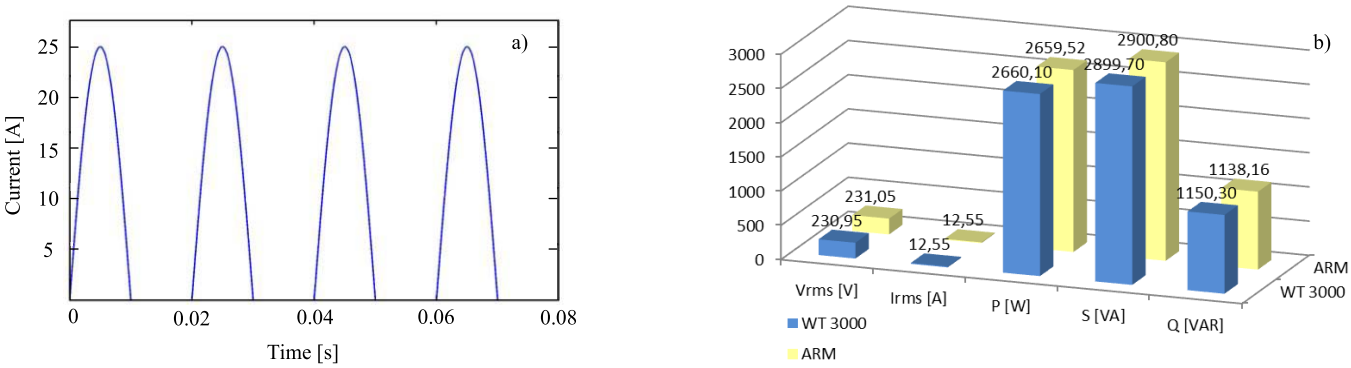

Fig. 10. DC and even harmonic in the a.c. electric current circuit: a) the considered electric current test signals and b) the corresponding obtained results.

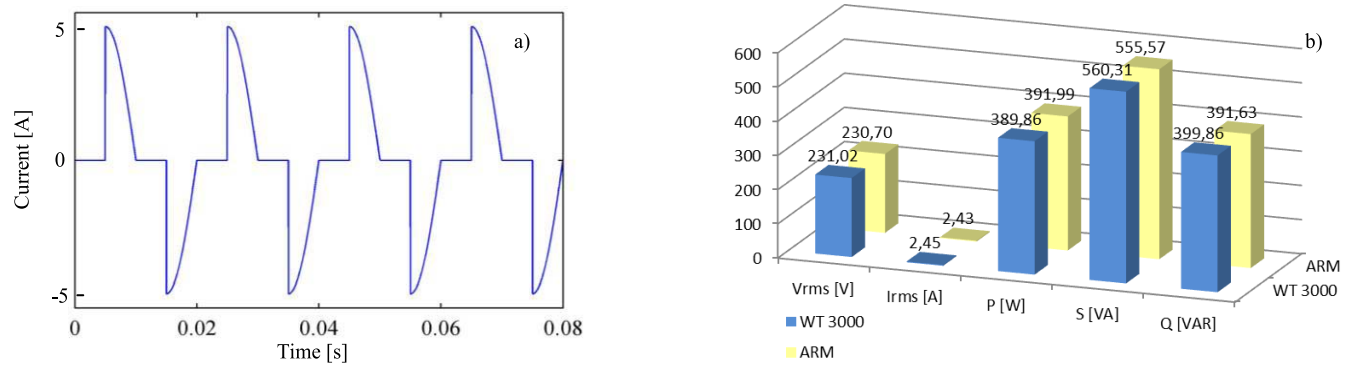

Fig. 11. Odd harmonic in the a.c. electric current circuit: a) the considered electric current test signals and b) the corresponding obtained results.

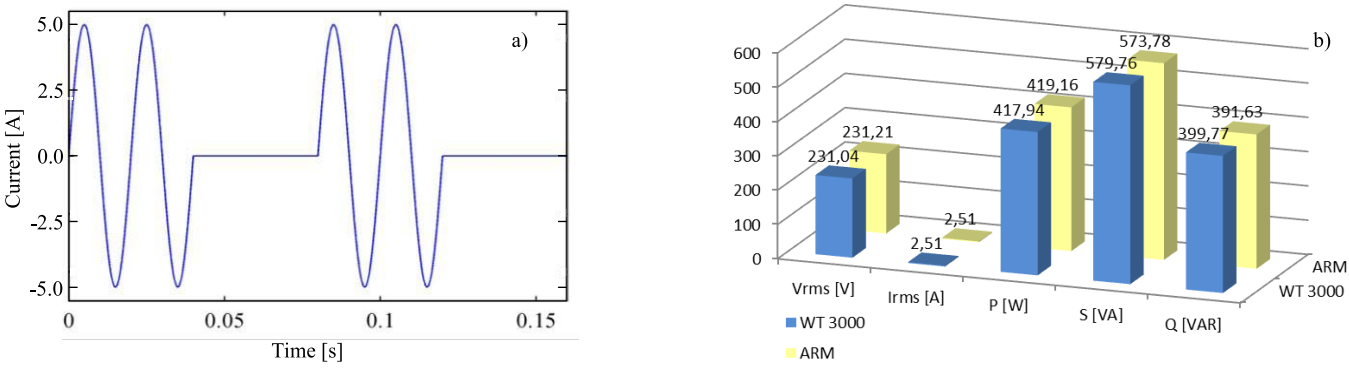

Fig. 12. Sub-harmonics in the a.c. electric current circuit: a) the considered electric current test signals and b) the corresponding obtained results.

The considered test waveforms have been generated via the Pacific 305AMX and 360AMX. Then the values measured with the prototype meter have been compared to the ones measured by the reference power analyzer Yokogawa WT3000.

For each test case, figures 8 to 12 show the obtained results in terms of comparison between the electrical energy parameters measured by the proposed ARM-based smart meter and that measured by the WT 3000 reference instrument.

TABLE I
MEAN VALUE AND STANDARD DEVIATION OF A SET OF MEASUREMENTS FOR DIFFERENT SIGNALS

	Sinusoidal Signals		Harmonics in voltage and electric current		DC and even harmonic		Odd harmonic in the a.c. electric current		Sub-harmonics in the a.c. electric current	
	Mean	Std	Mean	Std	Mean	Std	Mean	Std	Mean	Std
Vrms[V]	230.78	0.49	230.99	0.51	231.05	0.53	230.7	0.5	231.21	0.55
Irms[A]	4.971	0.021	12.422	0.043	12.551	0.042	2.431	0.015	2.510	0.011
P[W]	584.0	2.7	2760	11	2659.5	10.7	391.9	2.5	419.1	2.0
S[VA]	1146.8	5.4	2861	11	2900.8	11.7	555.5	3.6	573.7	2.8
Q[Var]	986.8	6.0	758	16	1138.1	15.9	391.6	4.4	391.6	3.5

In particular, the comparison was made respect to the root mean square of both voltage (Vrms) and electric current (Irms), active power (P), apparent power (S), and non-active power (Q).

For all the considered test cases, the values measured by the ARM-based smart meter for Vrms, Irms, P, and S are within the 1 % range respect to the measurements provided by the reference instrument. A greater error was revealed in the measurement of non-active power except in the sinusoidal test case (see figure 8b). Some improvements should be adopted to reduce this gap.

In the table I mean values and standard deviations for electrical quantity of interest computed on 30 repetitions of each test case. By considering the all the exanimated conditions according the OIML R-46 the developed meter belongs to class B.

VI. CONCLUSIONS

An ARM-based smart sensor unit has been developed and tested to be used in local area grids within a multi-level hierarchical architecture. A software module based on IEEE 1451 has been developed to add TIM and NCAP capability to unit. The unit acquires and processes information for three energy categories (electricity, gas and water). Indeed, the unit processes the voltage and electric current signals to provide active and non-active power measurements, together with information regarding power quality and usage statistics. These data are available on site for the user and can be sent to upwards in the network. The unit has been also designed to receive, alongside the interconnection network, commands relative to the DSM. The paper describes an original solution to reduce he effect of the main influence parameters on the measurement of electrical quantity, such as power grid frequency. Finally, the metrological characterization is reported. Verification tests conducted accordingly to MID and OIML R-46, in comparison with a reference instrument, allow to classify the developed prototype as class B electrical meter.

APPENDIX A
THE GOERTZEL ALGORITHM

To compute individual DFT coefficients the Goertzel Algorithm can be used.

Given k_i the index of the spectral component, f_i, to be measured $k_i = \frac{f_i}{\Delta f} = N \cdot \frac{f_i}{f_s}$, where Δf is the frequency resolution, N the total number of points of the DFT and f_S the sampling frequency, the $X(k_i)$ the spectral component of a input signal x(t) is evaluated as:

$$X(k_i) = \sum_N x(n) \cdot e^{-jk_i \frac{2\pi n}{N}}. \tag{A1}$$

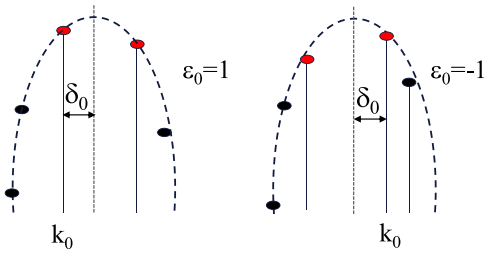

Fig. 13. The interpolation for estimation of the grid frequency.

APPENDIX B
THE FUNDAMENTAL FREQUENCY DETERMINATION

The Goertzel algorithm is applied to five frequencies near 50 Hz (40 Hz, 45 Hz, 50 Hz, 55 Hz, 60 Hz) for both electric current and voltage. The corresponding spectrum modules, $M(k_0)|_h$ (h states for I and V, electric current and voltage respectively), are calculated, then the modules of the voltage are analyzed to search for the maximum of the fundamental lobe, and finally an interpolation algorithm is applied in order to calculate the fundamental frequency, f_0.

The fundamental frequency is obtained as

$$f_1 = \Delta f \cdot (k_0 + \varepsilon_0 \cdot \delta_0),$$

where k_0 is the index of the maximum, and δ_0 is:

$$\delta_0 = \frac{\alpha}{1+\alpha}; \alpha = \frac{M(k_0 + \varepsilon_0)|_V}{M(k_0)|_V};$$

$$\text{Where } \varepsilon_0 = \begin{cases} 1 if\ M(k_0+1)|_V \geq M(k_0-1)|_V \\ -1 if\ M(k_0-1)|_V > M(k_0+1)|_V \end{cases}$$

Moreover, the interpolation allows evaluating the rms values for both electric current and voltage.

$$I_1^{rms} = \sqrt{2} \cdot \frac{\pi \cdot (1-\delta^2)}{\delta_0 \cdot \sin \pi \delta_0} \cdot M(k_0)|_I$$

$$V_1^{rms} = \sqrt{2} \cdot \frac{\pi \cdot (1-\delta^2)}{\delta_0 \cdot \sin \pi \delta_0} \cdot M(k_0)|_V$$

The phase difference is equal to the difference of measured phases of electric current and voltage at the spectral component k_0.

The significance of the used quantities are showed in Fig. 13.

REFERENCES

[1] Y. Cheng and L. Zhang, "Dynamic response model between power demand and power tariff," in *Proc. Int. Conf. Power Syst. Technol.*, vol. 2. Nov. 2004, pp. 1416–1421.

[2] A. Vos, "Effective business models for demand response under the smart grid paradigm," in *Proc. IEEE/PES Power Syst. Conf. Expo. (PSCE)*, Mar. 2009, p. 1.

[3] C. Chen, K. G. Nagananda, G. Xiong, S. Kishore, and L. V. Snyder, "A communication-based appliance scheduling scheme for consumer-premise energy management systems," *IEEE Trans. Smart Grid*, vol. 4, no. 1, pp. 56–65, Mar. 2013.

[4] K. M. Tsui and S. C. Chan, "Demand response optimization for smart home scheduling under real-time pricing," *IEEE Trans. Smart Grid*, vol. 3, no. 4, pp. 1812–1821, Dec. 2012.

[5] K. Ma, T. Yao, J. Yang, and X. Guan, "Residential power scheduling for demand response in smart grid," *Int. J. Elect. Power Energy Syst.*, vol. 78, pp. 320–325, Jun. 2016.

[6] G. Xiong, C. Chen, S. Kishore, and A. Yener, "Smart (in-home) power scheduling for demand response on the smart grid," in *Proc. ISGT*, Jan. 2011, pp. 1–7.

[7] A. B. Haney, T. Jamasb, and M. G. Pollitt, "Smart metering and electricity demand: Technology, economics and international experience," Cambridge Working Paper in Economics 0905, Faculty Econ., Univ. Cambridge, Cambridge, U.K., Tech. Rep., 2009.

[8] G. Stribac *et al.*, "Benefits of advanced smart metering for demand response based control of distribution networks," Centre Sustain. Electr. Distrib. Generat. Imperial College, London, U.K., Tech. Rep., Apr. 2010.

[9] G. Del Prete, D. Gallo, C. Landi, and M. Luiso, "Real-time smart meters network for energy management," *ACTA IMEKO*, vol. 2, no. 1, pp. 40–48, 2013.

[10] D. Di Cara, M. Luiso, G. Miele, and P. Sommella, "A smart measurement network for optimization of electrical grid operation," in *Proc. 19th IMEKO TC4 Symp.-Meas. Elect. Quantities 17th Int. Workshop ADC DAC Modelling Test.*, Jul. 2013, pp. 649–654.

[11] S. Grijalva and M. U. Tariq, "Prosumer-based smart grid architecture enables a flat, sustainable electricity industry," in *Proc. IEEE PES Innov. Smart Grid Technol. (ISGT)*, Jan. 2011, pp. 1–6.

[12] F. Li and P. Xiong, "Practical secure communication for integrating wireless sensor networks into the Internet of Things," *IEEE Sensors J.*, vol. 13, no. 10, pp. 3677–3684, Oct. 2013.

[13] H. Serra, J. Correira, A. J. Gano, A. M. de Campos, and I. Teixera, "Domestic power consumption measurement and automatic home appliance detection," in *Proc. IEEE Int. Workshop Intell. Signal Process.*, Faro, Portugal, Sep. 2005, pp. 128–132.

[14] M. De Santo, L. Ferrigno, V. Paciello, and A. Pietrosanto, "Experimental characterization of synchronization protocols for wireless networks," in *Proc. IEEE Conf. Virtual Environ., Hum.-Comput. Interfaces Meas. Syst. (VECIMS)*, Istanbul, Turkey, Jul. 2008, pp. 62–67.

[15] L. Ferrigno, V. Paciello, and A. Pietrosanto, "A Bluetooth-based proposal of instrument wireless interface," *IEEE Trans. Instrum. Meas.*, vol. 54, no. 1, pp. 163–170, Feb. 2005.

[16] L. Ferrigno, A. Pietrosanto, and V. Paciello, "Low-cost visual sensor node for BlueTooth-based measurement networks," *IEEE Trans. Instrum. Meas.*, vol. 55, no. 2, pp. 521–527, Apr. 2006.

[17] L. Ferrigno, V. Paciello, and A. Pietrosanto, "Visual sensors for remote metering in public networks," in *Proc. IEEE Instrum. Meas. Technol. Conf. (I2MTC)*, May 2011, pp. 1006–1011.

[18] G. Di Leo, M. Landi, V. Paciello, and A. Pietrosanto, "Smart metering for demand side management," in *Proc. IEEE Instrum. Meas. Technol. Conf. (I2MTC)*, Graz, Austria, May 2012, pp. 1798–1803.

[19] *Active Electrical Energy Meters. Part 1: Metrological and Technical Requirements. Part 2: Metrological Controls and Performance Tests*, document OIML R-46, 2012.

[20] C. Rottondi, G. Verticale, and C. Krauß, "Secure distributed data aggregation in the automatic metering infrastructure of smart grids," in *Proc. IEEE Int. Conf. Commun. (ICC)*, Jun. 2013, pp. 4466–4471.

[21] S.-W. Luan, J.-H. Teng, S.-Y. Chan, and L.-C. Hwang, "Development of an automatic reliability calculation system for advanced metering infrastructure," in *Proc. 8th IEEE Int. Conf. Ind. Inform.*, Jul. 2010, pp. 342–347.

[22] T. Uehara *et al.*, "System frequency control using emergency demand response in power systems with large-scale renewable energy sources," in *Proc. IEEE Region 10 Conf. (TENCON)*, Nov. 2016, pp. 534–537, doi: 10.1109/TENCON.2016.7848057.

[23] F. Abate, V. K. L. Huang, G. Monte, V. Paciello, and A. Pietrosanto, "A comparison between sensor signal preprocessing techniques," *IEEE Sensors J.*, vol. 15, no. 5, pp. 2479–2487, May 2015.

[24] *IEEE Standard for a Smart Transducer Interface for Sensors and Actuators-Network Capable Application Processor (NCAP) Information Model*, IEEE Standard 1451.1-1999, 2000.

[25] S. Fryze, "Active reactive and apparent power in circuits with non-sinusoidal voltage and current," *Electrotechn. J.*, vol. 53, no. 25, pp. 596–599, 1932.

[26] L. S. Czarnecki, "Two frameworks for interpreting power properties of circuits with nonsinusoidal voltages and currents," *Elect. Eng.*, vol. 80, no. 6, pp. 359–367, 1997.

[27] A. E. Emanuel, *Power Definitions and the Physical Mechanism of Power Flow*. Hoboken, NJ, USA: Wiley, 2010.

[28] A. Ferrero and G. Superti-Furga, "A new approach to the definition of power components in three-phase systems under nonsinusoidal conditions," *IEEE Trans. Instrum. Meas.*, vol. 40, no. 3, pp. 568–577, Jun. 1991.

[29] *IEEE Standard Definitions for the Measurement of Electric Power Quantities Under Sinusoidal, Nonsinusoidal, Balanced, or Unbalanced Conditions*, IEEE Standard 1459-2010, Mar. 2010.

[30] A. V. Oppenheim and R. W. Schafer, *Discrete-Time Signal Processing*, 2nd ed. Englewood Cliffs, NJ, USA: Prentice-Hall, 1999.

[31] C. Liguori, A. Paolillo, and A. Pignotti, "Estimation of signal parameters in the frequency domain in the presence of harmonic interference: A comparative analysis," *IEEE Trans. Instrum. Meas.*, vol. 55, no. 2, pp. 562–569, Apr. 2006.

[32] *Directive on Measuring Instruments (MID), European Parliament and of the Council*, Standard EU 2004/22/CE, 2004.

[33] *Electricity Metering Equipment (A.C.)—Part 3: Particular Requirements—Static Meters for Active Energy (Class Indexes A, B and C)*, Standard EN 50470-3, 2006.

Vincenzo Paciello (M'08–SM'13) was born in Salerno, Italy, in 1977. He received the M.S. degree in electronic engineering and the Ph.D. degree in information engineering from the University of Salerno, Fisciano, in 2002 and 2006, respectively. From 2008 to 2016, he was an Assistant Professor of Electrical and Electronic Measurements with the Department of Industrial Engineering, University of Salerno. Since 2016, he has been an Associate Professor of Electrical and Electronic Measurements with the Department of Electrical and Information Engineering, University of Cassino. He develops activity of referee for some prestigious international journals and for the evaluation of national and European research projects. His current research interests include mechanical and electronic measurements, wireless sensor networks, instrument interfaces, smart meter, smart sensor network, and digital signal processing for advanced instrumentation.

Antonio Pietrosanto (M'99–SM'12) was born in Naples, Italy, in 1961. He has been a Full Professor of electrical and electronic measurement, University of Salerno, since 2001. He is the Founder of three spin-offs of the University of Salerno: SPRING OFF, Metering Research, and Hippocratica Imaging. He has co-authored more than 150 papers in international journals and conference proceedings. His main research activities are in the fields of instrument fault detection and isolation, sensors, WSNs, real-time measurements, embedded systems, metrological characterization of measurement software, advanced system for food quality inspection, and image-based measurements.

Paolo Sommella (M'11) was born in Salerno, Italy, in 1979. He received the M.S. degree in electronic engineering and the Ph.D. degree in information engineering from the University of Salerno, Italy, in 2004 and 2008, respectively. In 2015, he joined the Department of Industrial Engineering, University of Salerno, as an Assistant Professor of Electrical and Electronic Measurements. His main interests are instrument fault detection and isolation, measurement in software engineering, biomedical image processing, and smart meter technology.